

Electronic Supplementary Material (ESI) for Journal of Materials Chemistry C. This journal is ©

The Royal Society of Chemistry 2022

Supporting Information

Sandwich-type phase change composites with dual-function of efficient heat management and temperature-regulated electromagnetic interference shielding performance

Ling Qin,^{‡abc} Cui Liu,^{‡bc} Jixiang Zhang,^{*abc} Min Xi,^{bc} Shuai Pi,^{abc} Wei Guo,^{bc} Nian Li,^{*bc} Shudong Zhang,^{*bc} and Zhenyang Wang^{*bc}

^a *School of Mechatronics and Vehicle Engineering, Chongqing Jiaotong University, Chongqing 400074, China*

^b *Institute of Solid State Physics, Hefei Institutes of Physical Science, Chinese Academy of Sciences, Hefei, Anhui, 230031, China.*

^c *Key Laboratory of Photovoltaic and Energy Conservation Materials, Hefei Institutes of Physical Science, Chinese Academy of Sciences, Hefei 230031, China*

*** Corresponding Authors.**

Jixiang Zhang. E-mail: jixiangzhang@163.com

Nian Li. E-mail: linian@issp.ac.cn

Shudong Zhang. E-mail: sdzhang@iim.ac.cn;

Zhenyang Wang. E-mail: zywang@iim.ac.cn;

S1 Experimental section

S1.1 Materials

Expanded graphite (EG), average particle size 50 mesh, purchased from Qingdao Tengshengda carbon graphite. Multiwalled carbon nanotubes (MWCNTs) are purchased from Nanjing Jicang Nanotechnology Co., Ltd. Octane (ES, $\rho=0.8\pm 0.1\text{g/cm}^3$, melting point 35-37°C) was purchased from Shanghai Aladdin Biochemical Technology Co., Ltd. Polyvinylidene fluoride (PVDF, molecular weight $N_w = 1$ million) was purchased from Zhanyang Polymer Company, Dongguan. Iron oxide (II, III) (Fe_3O_4 , 50 - 150 nm) was provided from Aladdin Chemistry Co. Ltd., China.

S1.2 Characterizations

Cu-K α radiation (40 KV, 30 mA) was used at room temperature, and the scanning speed was 10°/min. The crystal structures of the materials from 10° to 90° were recorded by X-ray diffraction (XRD, X'Pert, PANalytical, Netherlands). Scanning electron microscopy (SEM, SU8020, Hitachi, Japan) was used to observe the microstructure at 5KV accelerating voltage. Before SEM testing, all surfaces were sputtered with gold to provide enhanced conductivity. Differential scanning calorimetry (DSC, DSC-Q2000, TA Instrument Company, USA) was used to test the phase transition temperature and latent heat in the range of 0°C to 80°C at 10°C/min. The uncertainty of DSC measurement for temperature and enthalpy was 0.05°C and 3.0%, respectively. Thermogravimetric analyzer (TGA, SDT650, TA Discovery, USA) was used to heat from 25°C to 600°C at 10°C/min in nitrogen atmosphere. The thermal diffusivity of each sample was measured by a laser thermal conductivity meter (LFA 457, NETZSCH, Germany). The thermal conductivity was calculated by the formula, where D is the thermal diffusivity, ρ is the density, and C_p is the constant pressure specific heat capacity. The volume conductivity was measured by a four-probe

instrument (ST2258C, Suzhou Lattice Electronics Co., Ltd.). Each sample was tested at four different points, and the average value of the results was taken. At room temperature, the magnetic measurement system (MPMS XL5, Quantum Design, USA) was used to test the magnetization of Blend and PVDF/Fe₃O₄ spinning membrane with Fe₃O₄. The electromagnetic interference of samples in X-band (8.2-12.4GHz) was measured by vector network analyzer using waveguide method. Thermal management performance of sandwich structure materials is recorded by infrared thermal imager (Fluke Tis75, USA). Thermal cycling test was carried out in a dry incubator (JX-20, Shanghai Jingxin Industrial Development Co., Ltd.) between 20°C and 70°C.

S2 Results and discussions

S2.1 Attribution of diffraction peaks

According to Fig. S1A, the diffraction peak at $2\theta=27^\circ$ in PCCs belongs to the result of the interaction between eicosane and expanded graphite. Compared with the crystal plane at $2\theta=27.06^\circ$ (111) of eicosane, it has a slight left shift. The diffraction peak $2\theta=26.56^\circ$ of the expanded graphite belongs to the (002) crystal plane, and the similar diffraction peak $2\theta=26^\circ$ corresponds to the characteristic peak of the (002) crystal plane of the multi-walled carbon nanotubes belonging to the graphite. The peaks $2\theta=20.1^\circ$, 24.15° and 27.06° of n-octadecane belong to (010), (100) and (111) crystal planes, respectively.

S2.2 XRD of PCCs

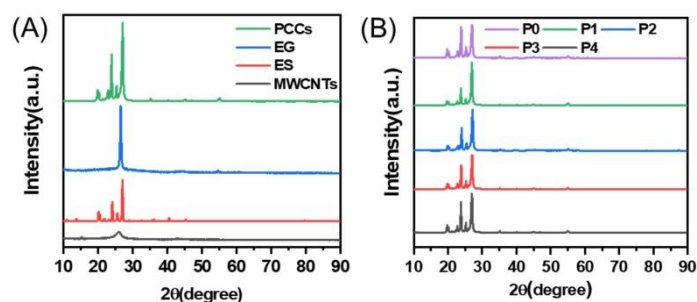


Fig.S1 (A) XRD of PCCs, EG, ES and MWCNTs. (B) XRD of P0, P1, P2, P3, P4.

S2.3 SEM and EMI SE of Magnetic spinning film (MSF)

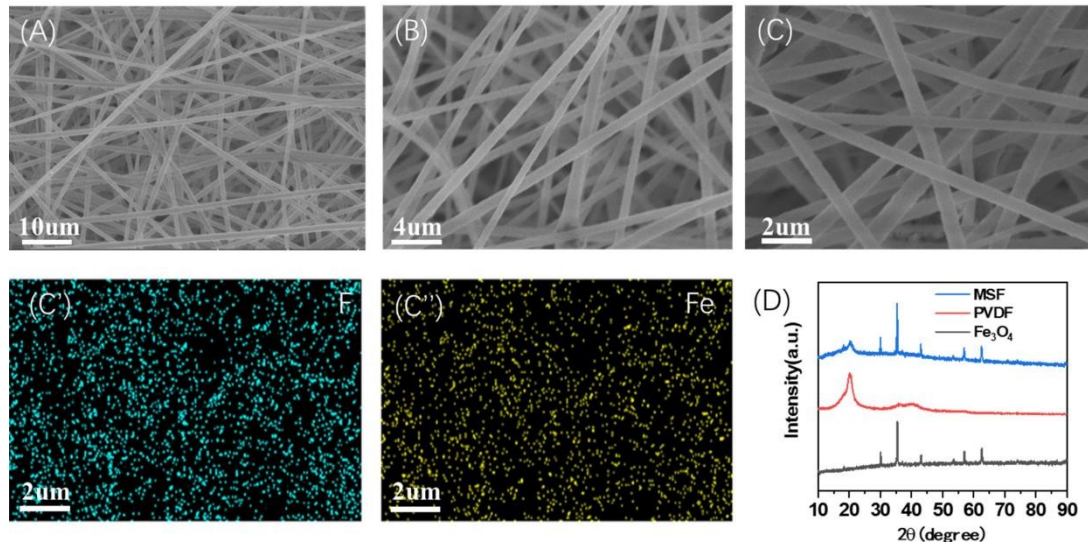


Fig.S2 (A-C) SEM images of Magnetic spinning film (MSF), (C', C'') EDS mapping of elements F and Fe, (D)

XRD of MSF, Fe_3O_4 and PVDF.

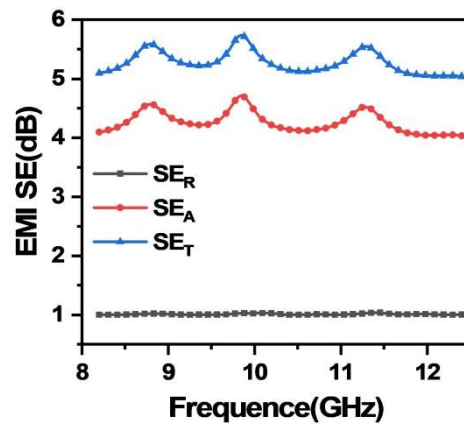


Fig.S3 EMI SE of MSF.

S2.4 Magnetism of MSF, BC and Fe_3O_4

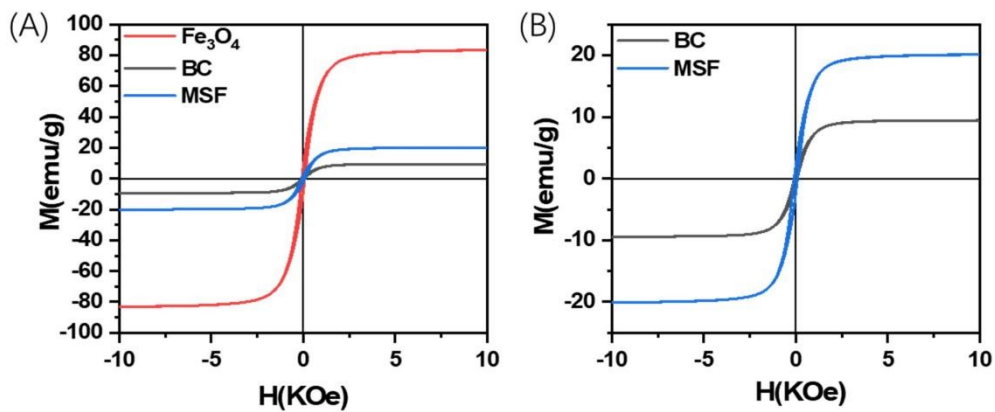


Fig. S4 (A) Field dependent magnetization curves of Fe_3O_4 , BC and MSF. (B) Field dependent magnetization curves of BC and MSF.

S2.5 SEM and EDS of BC

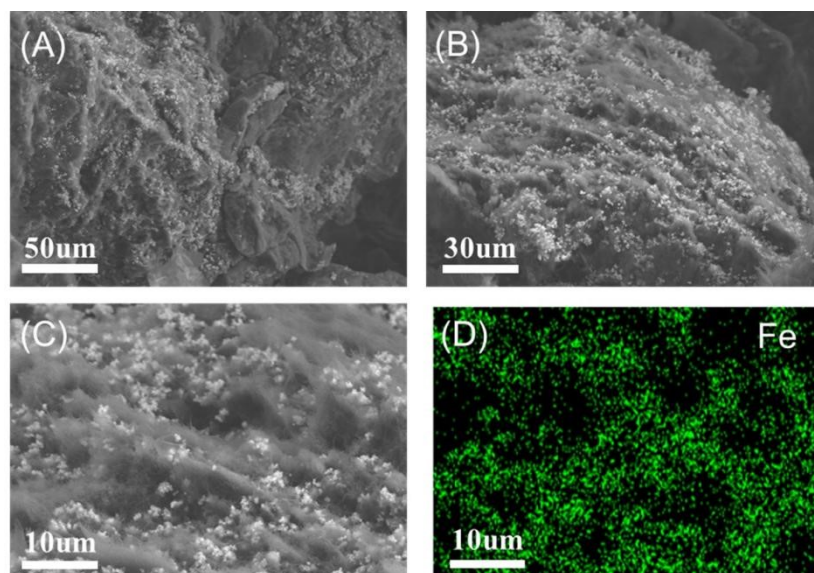


Fig. S5 (A-C) SEM images of BC, (D) EDS mapping of elements Fe.

S2.6 Heat-resistance index (THRI) values of ES and STPCCs

Table.S1 Heat-resistance index (THRI) values of ES and STPCCs

Samples	Weight loss temperature/°C		THRI */ °C
	T ₅	T ₃₀	
ES	167.9	211.5	95.1
SC0	179.2	222.2	100.5
SC1	185.4	225.3	102.6
SC2	184.6	224.6	102.2
SC3	185.4	225.3	102.6
SC4	180.8	228.2	102.5

*Heat-resistance index = $0.49 \times [T_5 + 0.6 \times (T_{30} - T_5)]$. T₅ and T₃₀ represent the corresponding decomposition temperatures of 5 wt% and 30 wt% weight loss, respectively.

S2.7 Shape stability of ES, PCCs, STPCCs, and BC

$$\omega = \frac{m_1 - m_n}{m_1} \times 100\%$$

m₁ is the initial weight of the sample and m_n is the weight of the sample after each time it is kept for a

certain heating time.

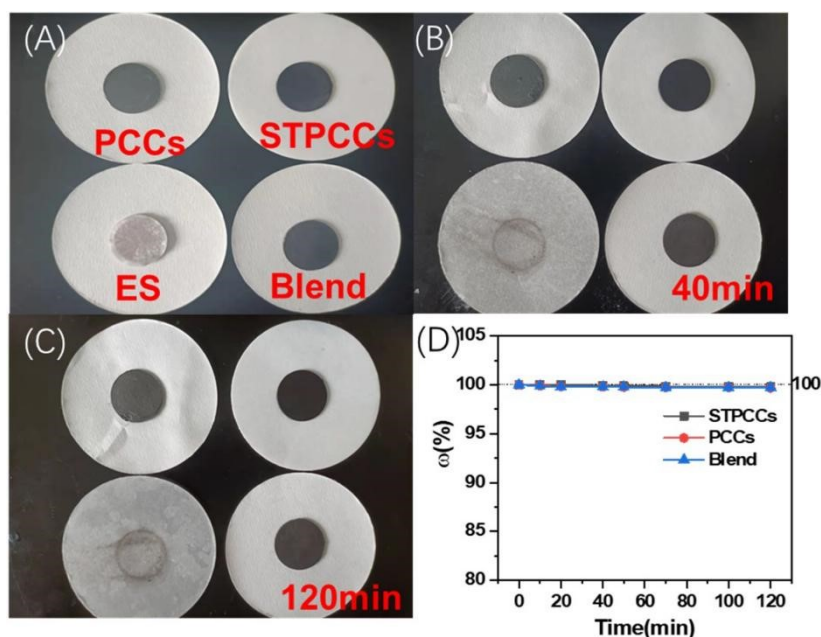


Fig. S6 (A-C) Digital photos of ES, PCCs, STPCCs, and BC maintained at 70°C in an oven for 2 hours, (D) Weight statistics of ES, PCCs, STPCCs, and BC during leakage experiments

S3 The EMI shielding and Thermal conductivity properties of the reported works.

Table.S2 The EMI shielding properties of the reported works

Materials	Thick/mm	SE _T /dB	Thermal conductivity (W/mK)	Ref.
PP/CNTs/Fe ₃ O ₄ /PW	2	39.2	0.59	1
WPC/PEG/Fe ₃ O ₄	4.91	55.09	-	2
MXene/PCM	3	64.7	0.74	3
PW@CNS	3	29.4	1.85	4
Scaffold/PW	1.5	37.7	0.38	5
MF@MA/PEG	2	30.5	0.196	6
MPA χ -PEG PCM	1.5	82.02	0.42	7
NiM/PCM	2	34.6	0.39	8
PP/CNT&EPDM/PW SSPCC	1	57.2	0.469	9
MSF/PCCs/MSF	1	98.39	3.61	This word

Reference

- 1 X.L. Li, M.J. Sheng, S Gong, H Wu, X.L. Chen, X Lu and J.P. Qu, *Chemical Engineering Journal*, 2022, **430**, 132928.
- 2 S Liu, M.J. Sheng, H Wu, X.T. Shi, X Lu and J.P. Qu, *Journal of Materials Science & Technology*, 2022, **113**, 147-157.
- 3 H. Liu, R.L. Fu, X.Q. Su, B.Y. Wu, H Wang, Y Xu and X.H. Liu, *Composites Science and Technology*, 2021, **210**, 108835.
- 4 X Lu, Y.F. Zheng, J.L. Yang and J.P. Qu, *Composites Part B: Engineering*, 2020, **199**, 108308.
- 5 M Zhou, J.W. Wang, Y Zhao, G.H. Wang, W.H. Gu and G.B. Ji, *Carbon*, 2021, **183**, 515-524.
- 6 Y.J. He, Y.W. Shao, Y.Y. Xiao, J.H. Yang, X.D. Qi and Y Wang, *ACS Applied Materials & Interfaces*, 2022, **14**, 6057 - 6070.

- 7 Y.Y. Xiao, Y.J. He, R.Q. Wang, Y.Z. Lei, J.H. Yang, X.D. Qi and Y Wang, *Composites Part B: Engineering*, 2022, **239**, 1359-8368.
- 8 H.R. Cheng, L.L. Xing, Y Zuo, Y.M. Pan and M.N. Huang, *Advanced Composites and Hybrid Materials*, 2022, **5**, 755-765
- 9 X.P. Hu, C.B. Zhu, B.Q. Quan, M.J. Sheng, H Wu, X Lu and J.P. Qu, *Chemical Engineering Journal*, 2022, **446**, 137423.
- 10 Y. Liang, Y. Tong, Z. Tao, Q. Guo, B. Hao and Z. Liu, *Macromolecular Materials and Engineering*, 2021, **306**, 210055.